Proceedings of the 21st ICSMGE, Vienna, Austria, 14 – 19 June 2026. Pistrol, Adam & Schweiger (eds.)
Published by: ÖGG, Austrian Society for Geomechanics, Salzburg, Austria, ISBN 978-3-9503898-4-5
https://doi.org/10.53243/ICSMGE2026-1691

In-situ estimation of a pseudo-3D model of shear wave velocity and small strain damping ratio at a downhole seismic array site using surface wave testing

Mauro Aimar, Sebastiano Foti
Dept. of Structural, Building and Geotechnical Engineering, Politecnico di Torino, Torino, Italy, mauro.aimar@polito.it

Aser Abbas
Dept. of Civil and Environmental Engineering, The University of Rhode Island, Kingston, USA

Nishkarsha Dawadi, Brady R. Cox
Dept. of Civil and Environmental Engineering, Utah State University, Logan, USA

ABSTRACT: Reliable three-dimensional (3D) in situ characterization of the subsurface small-strain shear modulus (G_0) and small-strain damping ratio (D_0) is paramount for quantifying the response of soil deposits to seismic loading. The small-strain parameters strongly influence low-amplitude shaking and anchor soil nonlinear behavior during strong shaking. In this study, active-source and ambient-noise surface wave measurements are used to estimate a site-specific, large-scale, pseudo-3D model of both shear wave velocity (V_S) and D_0 at a downhole seismic array site in the United States. The combination of active-source and ambient-noise vibrations enables good near-surface resolution and deep subsurface characterization. When paired with a large number of spatially distributed Horizontal-to-Vertical (H/V) spectral ratio measurements, this approach allows for pseudo-3D site characterization of both V_S and D_0 over an area compatible with the large spatial area that influences seismic site response. Incorporating spatial variability of the soil parameters in this way can help to capture complex wave propagation phenomena (e.g., wave scattering) that are not included in conventional, 1D ground response modelling. The resulting pseudo-3D subsurface model can then be used in 3D ground response analyses at the downhole array site in an attempt to better match the recorded site response amplifications from small-strain aftershock ground motions.

KEYWORDS: Site characterization, Shear wave velocity, Damping ratio, Surface wave methods, Site response.

1 INTRODUCTION

Assessing the seismic hazard for critical infrastructure requires evaluating the site-specific influence of subsoil conditions on the amplitude and frequency content of earthquake ground motions (GMs), a phenomenon commonly referred to as site effects. This is achieved through ground response analysis (GRA), which numerically simulates how earthquake GMs are modified as they propagate from bedrock to the ground surface. One common method to evaluate the accuracy of GRAs is by computing the numerically-based, theoretical transfer function (TTF), defined as the ratio of the Fourier amplitude spectra of horizontal surface accelerations to those at a deeper rock layer. This TTF is then compared to the empirical transfer function (ETF) from downhole array sites, where both input (rock) and output (surface) GMs are recorded. Over the past two decades, considerable research has sought to improve GRA predictive accuracy using these downhole array sites as benchmarks for model performance (e.g., Teague et al., 2018). Although some studies have successfully replicated observed site responses at certain locations, they fail to do so at approximately 50% of downhole array sites (Hallal et al., 2022). Moreover, even the successful predictions typically match only the frequency of the fundamental mode, often overestimating its amplification (i.e., amplitude) and rarely capturing higher modes in terms of either frequency, amplitude, or both. Two primary challenges that limit our ability to accurately model site effects are: (1) inaccuracies in characterizing the dynamic constitutive parameters of subsurface geomaterials, and (2) the common assumption of one-dimensional (1D) site conditions (Hallal and Cox, 2021b).

Regarding the first challenge, two relevant constitutive parameters controlling site effects are the small-strain shear modulus (G_0) and the small-strain damping ratio (D_0). These parameters primarily govern the amplification of low-amplitude ground motions, where the response can be effectively predicted using linear viscoelastic models, and anchor soil nonlinear behavior under strong shaking conditions. While considerable progress has been made over the past several decades in estimating G_0 in situ, primarily through advances in shear wave velocity (V_S) measurements, the in-situ estimation of D_0 remains significantly more challenging (Parolai et al., 2022). D_0 is typically inferred from empirical correlations (e.g., Darendeli, 2001) or measured in laboratory settings, both of which tend to underpredict damping in situ. As for the second challenge, GRAs commonly assume 1D site conditions, in which the subsurface is modeled as a series of horizontally layered, laterally homogeneous materials, and wave propagation is assumed to occur only in the vertical direction. These limitations can be mitigated by adopting 2D and 3D GRAs, which better capture the effects of irregular topography and lateral geological variations. Moving from 1D to 2D simulations significantly improves the modeling of ground motion amplification in complex geological settings. In some cases, such as elongated basins (e.g., valleys; Makra and Chávez-García, 2016), 2D analyses can provide estimates comparable to those of 3D simulations, although they fail to reproduce certain amplification patterns in more challenging conditions (e.g., Falcone et al., 2018). Consequently, recent research has increasingly focused on 3D GRAs. These offer a more realistic representation of subsurface conditions and earthquake ground shaking, but their application has been rare, largely because reliable and cost-effective 3D subsurface imaging, necessary for model development, remains a significant challenge. Moreover, 3D GRA simulations are significantly more computationally demanding than their 1D counterparts.

This study demonstrates recent advancements in 3D subsurface imaging of both G_0 and D_0 using in-situ, cost-effective, and efficient surface wave testing techniques. The resulting pseudo-3D model is then applied in a 3D GRA at a downhole array site in Salt Lake City, Utah, USA in attempts to replicate the ETF recorded by the array during the 2020 M5.7 Magna earthquake.

2 I-15 DOWNHOLE ARRAY SITE DESCRIPTION

The I-15 Downhole Array (I15DA; Youd and Briggs, 2003) is located near the junction of Interstates I-15 and I-80 in South Salt Lake City, Utah. The site lies within a seismically active region, approximately 5 km west of the Salt Lake City segment of the Wasatch Fault Zone and about 4 km east of the Taylorsville segment of the West Valley Fault Zone. The subsurface is composed of soft sediments deposited by the prehistoric Lake Bonneville, with bedrock expected at significant depth. The array consists of five, three-component force-balance accelerometers (FBAs): one at the ground surface and four at depths of 7.6 m, 18.3 m, 48.8 m, and 119.8 m. Each borehole was cased with PVC and grouted in place to ensure adequate sensor coupling and protection. Due to power loss and telemetry/data buffering issues, the array did not record the mainshock of the 2020 M5.7 Magna earthquake. However, both the surface and deepest sensors (119.8 m) successfully recorded several aftershocks.

The V_S profile at the site was initially characterized through cross-hole seismic testing and PS-logging, as documented by Youd and Briggs (2003). However, our team conducted active-source and ambient noise surface wave testing at the site with the goals of: (a) extending the V_S profile for the site to greater depths, and (b) recording a large number of spatially distributed horizontal-to-vertical (H/V) spectral ratio of noise measurements to facilitate development of a pseudo-3D V_S model at the site (Jackson 2024). Eventually, this same data was used to extract in-situ attenuation data and develop a pseudo-3D damping model at the site, as detailed below.

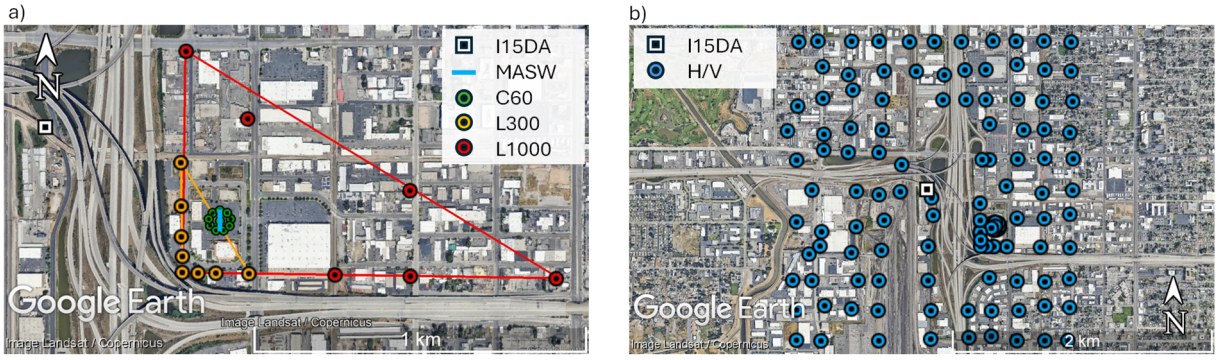

Figure 1. Map of the sensors' locations used for a) the MASW and the MAM testing, and b) H/V spectral ratio measurements at the I15DA site.

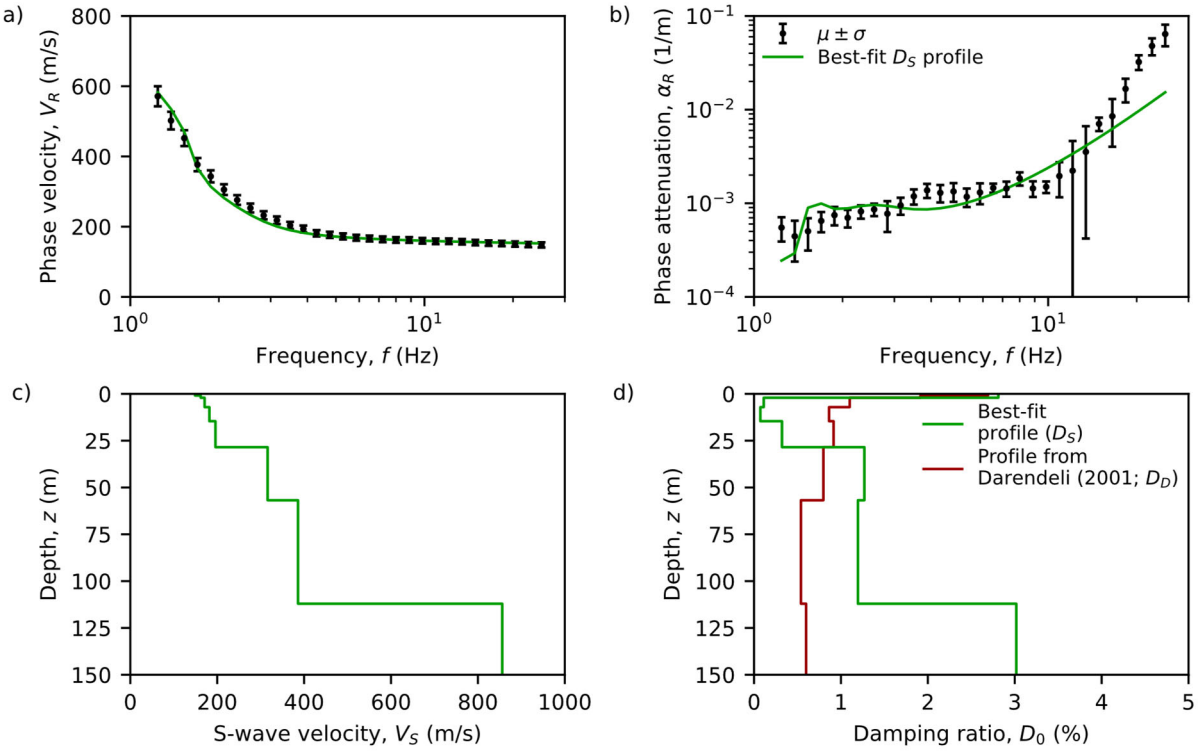

Figure 2. Estimation of the V_S and D_0 profile at the I15DA site from the MASW and MAM survey data: a-b) Estimated phase velocity and phase attenuation vs. frequency data, respectively, overlapped with the theoretical curves corresponding to the best-fit profile; c-d) Best-fit V_S and D_0 profile. The best-fit D_S profile in d) is compared with the corresponding empirical estimate according to Darendeli (2001). The phase velocity data in a) and the V_S profile in b) correspond to those derived in Jackson (2024).

3 SURFACE WAVE CHARACTERIZATION AT THE I15DA SITE

Site characterization was performed through a surface wave testing campaign based on active-source and ambient vibration array testing in an area next to the I15DA (Figure 1). Specifically, multichannel analysis of surface waves (MASW) was conducted using a linear array of 24, 4.5-Hz vertical geophones with 2 m spacing. The array was placed in a parking area, and the sensors were coupled to the paved surface using aluminum tripod bases. The active source was a sledgehammer striking on a metal plate. Source-offsets of 5, 10, and 20 m were used off both ends. Ambient vibration analysis was performed through two-dimensional microtremor array measurements (MAM). This involved one 60-m diameter circular array (labeled as "C60") centered in correspondence with the MASW array and two L-shaped arrays with an aperture of 300 m and 1,000 m, respectively (labeled "L300" and "L1000").

Each MAM array consisted of ten broadband seismometers that were buried in the ground whenever possible to improve coupling (Foti et al., 2018). Ambient vibration data were recorded for periods between 1.5 and 3 hours. In addition, single-station horizontal-to-vertical spectral ratio (H/V) measurements were performed at 96 different locations, forming an approximately 200 m × 200 m grid centered on I15DA (Figure 1b). At each H/V location, the sensors recorded ambient noise for approximately 30 minutes. The H/V measurements were used to estimate the natural frequency of the soil deposit ($f_{0,H/V}$) at the site and address site lateral variability. Most importantly, this represents the basis for the development of the pseudo-3D model, which will be discussed in the next section. Further details on the site characterization campaign can be found in Jackson (2024).

Both the MASW and the MAM data were used to estimate the 1D V_S and D_0 profiles at the site. First, surface wave data were processed to obtain the Rayleigh wave propagation parameters, expressed in terms of phase velocity and phase attenuation vs. frequency data (refer to Figure 2a,b). Active-source data were interpreted through the cylindrical frequency domain beamformer attenuation (CFDBFa) algorithm (Aimar et al., 2024a). Comparing data from different shots allowed us to identify and remove data potentially affected by near-field effects or incoherent noise, according to the multiple source-offset technique (Wood and Cox, 2012). As for MAM data, the noise frequency domain beamformer attenuation (NFDBFa) algorithm (Abbas et al., 2025) was used to extract the phase attenuation data from the vertical motion recordings. For this purpose, recordings from each array were divided into time windows with a length containing at least 30 cycles of the lowest frequency targeted. Spurious attenuation estimates were removed through manual trimming.

The individual phase velocity and phase attenuation data from MASW and MAM were combined to estimate the corresponding statistics (i.e., mean and standard deviation), which are reported in Figure 2a & 2b, respectively. These statistics were computed over a grid of 30 log-spaced frequencies ranging from 1.25 Hz to 25 Hz. Attenuation data beyond 25 Hz were not considered because they exhibited remarkably higher variability, presumably due to the influence of higher Rayleigh modes.

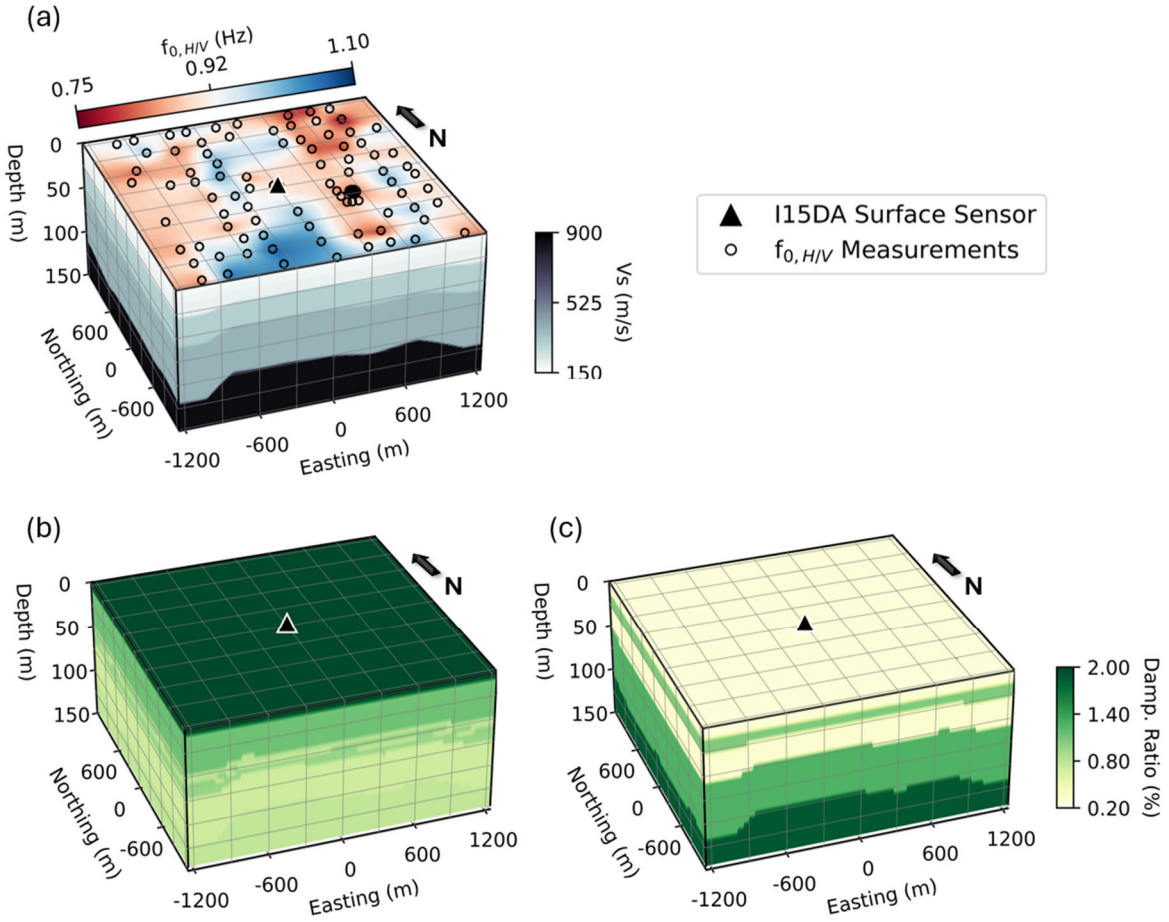

Figure 3. Pseudo-3D subsurface models at the I15DA site: (a) pseudo-3D shear wave velocity (V_S) model; (b) pseudo-3D damping ratio model based on the 1D damping profile at the downhole array computed using Darendeli's (2001) empirical equations; and (c) pseudo-3D damping ratio model derived from the 1D inversion-based damping profile at the same location.

Experimental phase attenuation data were inverted to estimate the 1D D_0 profile while using a simplified 1D, nine-layer V_S profile developed by Jackson (2024) as a constraint (refer to Figure 2c). The inversion was performed through a Monte Carlo-based, global search procedure that takes advantage of the scaling properties of the Rayleigh eigenvalue problem in linear viscoelastic media (Aimar et al., 2024b). The inversion was run generating 10,000 trial earth models. For simplicity, the P-wave damping ratio was assumed as equal to the S-wave value, whereas the remaining parameters (i.e., mass density and Poisson's ratio) matched those reported in Jackson (2024). These assumptions are based on the limited influence of these parameters on phase velocity and phase attenuation (e.g., Badsar, 2012; Foti et al., 2018) and help to mitigate the non-uniqueness of the solution to the surface-wave inversion problem. The forward modeling was conducted through the Computer Programs for Seismology software (Herrmann, 2013). The fit to the experimental data was quantitatively assessed using a normalized root mean square (RMS) error that accounts for estimation uncertainty (e.g., Wathelet et al., 2004). Figure 2d shows the lowest misfit 1D D_0 profile, which will be used for the rest of the study (label "D_S").

The corresponding theoretical attenuation curve is compared with the experimental data in Figure 2b. Figure 2a includes a similar comparison with the theoretical dispersion curve, proving that the 1D V_S profile inverted by Jackson (2024) is consistent with the experimental surface wave data. Furthermore, Figure 2d compares the inverted D_S profile with the profile obtained using the empirical formulas by Darendeli (2001), hereafter labeled as D_D. Notably, D_D is relatively constant and gradually decreases from 1% to 0.5% with the depth, primarily due to increased confining pressure. On the other hand, the inverted D_S is relatively high at the surface (~ 3%) and then decreases significantly (i.e., less than 0.5%) at intermediate depths due to the rather small experimental phase attenuation data in the 5–10 Hz frequency band. Then, D_S increases significantly again at greater depths, up to 3%. This large increase is mainly due to the large experimental phase attenuation at low frequencies. This may be due to the presence of a fine-grained soil formation underlying the downhole array, as suggested by the geological data available at the site (Jackson, 2024). Another possible reason behind the increase in the S-wave damping ratio could be the presence of additional dissipation mechanisms, such as wave scattering, induced by spatial variability and heterogeneities at the site. However, the limited information about the deep geology at the site does not allow to draw strong conclusions at this stage. Given the differences in the D_S and D_D profiles, both will be used to build the pseudo-3D models to investigate the impact of different damping ratio assumptions on the predicted site response and assess their consistency with observed ground motion amplification.

4 DEVELOPMENT OF PSEUDO-3D MODELS

The pseudo-3D V_S and D_0 models for the I15DA site were developed using the H/V Geostatistical Approach introduced by Hallal and Cox (2021a). This method was originally proposed for generating site-specific pseudo-3D V_S models by combining spatially distributed single-station H/V noise measurements, geostatistical optimization (kriging), and a V_S profile extending to the primary impedance contrast. The

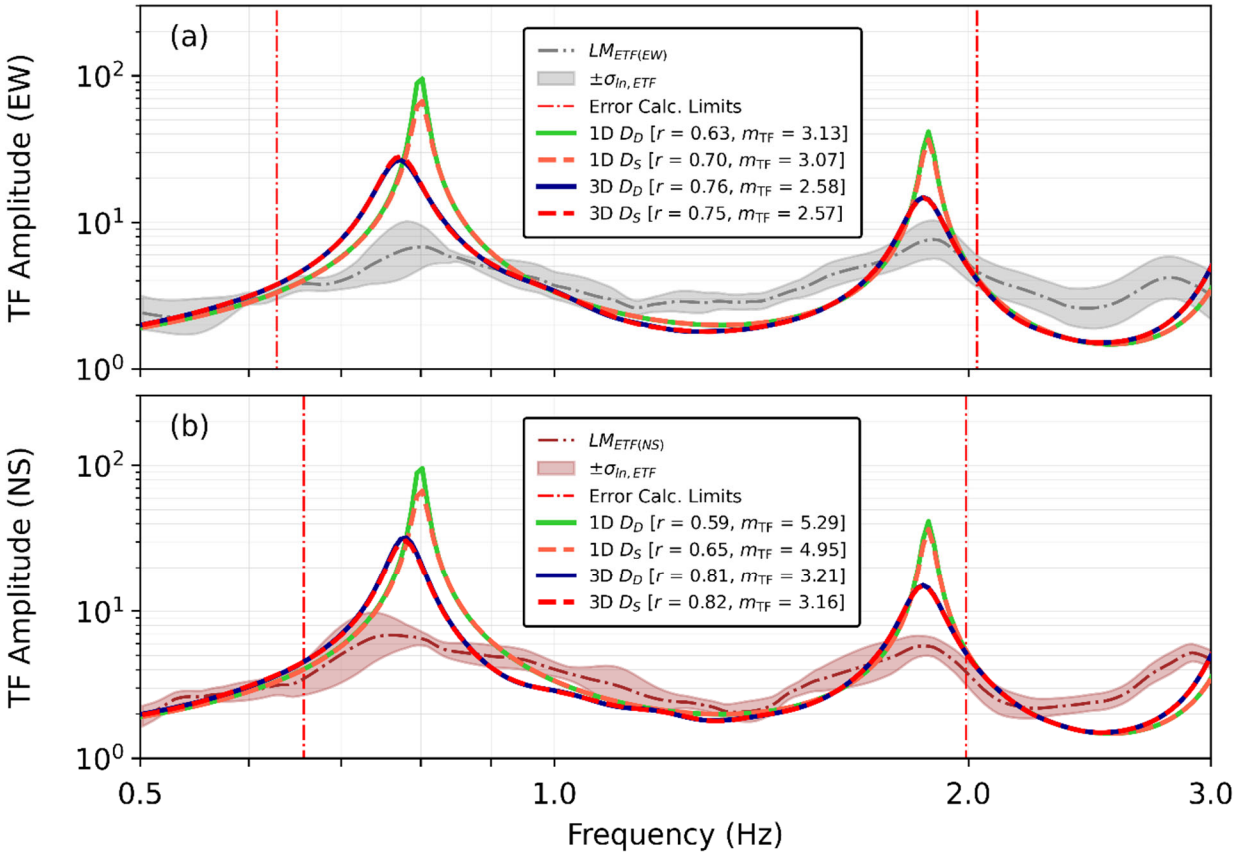

Figure 4. Results from 1D analytical and 3D numerical GRA at the I15DA site. Shown are comparisons between TTFs and ETFs for: (a) the EW component and (b) the NS component. The TTFs were obtained using two damping models: D_D (based on Darendeli's empirical equations) and D_S (based on inversion-derived damping). The Pearson correlation coefficient (r) and transfer function misfit (m_{TF}) values for each case are provided in the figure legends.

approach has been successfully applied to generate pseudo-3D V_S models at several downhole array sites, including the Treasure Island Downhole Array site (Hallal and Cox, 2021a), Delaney Park Downhole Array (Hallal and Cox, 2021a; Dawadi et al., 2024), and I15DA (Jackson, 2024; Dawadi et al., 2025a). In the present study, the base V_S profile obtained from deep surface wave testing conducted by Jackson (2024) at the I15DA and reported in Figure 2c was extrapolated across the model domain using the $f_{0,H/V}$ values obtained from the 96 single-station H/V measurements. The resulting pseudo-3D V_S model (Figure 3a) spans 2.5 km by 2.5 km horizontally, extends to a depth of 150 m, and consists of 7.5 million 5-m cubed elements. Additionally, two different pseudo-3D damping models were developed utilizing the same H/V Geostatistical framework by extending the D_S and the D_D profiles (Figure 3b and 3c, respectively).

To conduct 3D ground response analyses (GRAs) at the I15DA site, linear-viscoelastic ground response analyses were performed using FLAC-3D. The pseudo-3D V_S and D_0 models were directly assigned to the model zones, and a constant mass density of 2000 kg/m³ was assumed, because of its generally limited role on ground motion amplification and the presumable homogeneity in terms of mass density of the soil deposit, being composed mainly of an alternance of sands and clays, compared with other parameters (e.g., Rathje et al., 2010). Full Rayleigh damping was implemented, with quiet boundaries applied at the model base and free-field boundaries at the lateral edges. Because the present study focuses on linear-viscoelastic behavior, it was not necessary to use recorded ground motions. Instead, simulations were conducted using a combination of Ricker wavelets containing sufficient energy across the frequency range of interest, up to 3 Hz in this case, to capture both the fundamental and first higher-mode peaks.

5 GROUND RESPONSE ANALYSES AT THE I15DA SITE

The efficacy of the two damping models was evaluated by comparing numerically-based, theoretical transfer functions (TTFs), calculated as the ratio of the Fourier amplitude spectra (FAS) of the simulated motion at the surface to that at the 120 m downhole sensor, with empirical transfer functions (ETFs) developed by Jackson and Cox (2025) using small-strain recorded aftershock motions at the I15DA. Comparisons were made both visually and by using statistical metrics including the Pearson correlation coefficient (r) and the transfer function misfit (m_{TF}). Further details about r and m_{TF} can be found in Teague et al. (2018). Comparison of the simulated TTFs and observed ETFs were made both for the East-West (EW) and North-South (NS) components, as shown in Figure 4a and 4b, respectively

In the 1D GRAs, the inversion-based damping profile (i.e., D_S) produces noticeably lower amplitude peaks compared to the Darendeli-based damping profile (i.e., D_D) in both directions. Statistically, D_S also performs better: in the EW component, r increases from 0.63 to 0.70 and m_{TF} decreases from 3.13 to 3.07; in the NS component, r improves from 0.59 to 0.65 and m_{TF} drops from 5.29 to 4.95. These results suggest that the D_S profile yields better alignment with the observed ETF than the D_D profile under 1D assumptions.

In the 3D GRAs, the differences obtained by assuming the D_D and D_S pseudo-3D damping ratio models are not as significant, perhaps because the apparent damping caused by wave scattering in 3D is a more dominant factor. For the EW component (Figure 4a), D_S yields a slightly lower misfit ($m_{TF} = 2.57$ vs. 2.58), although its r value is marginally lower than that of D_D (0.75 vs. 0.76). For the NS component (Figure 4b), D_S performs better in both metrics, with r increasing from 0.81 (D_D) to 0.82 (D_S) and m_{TF} decreasing from 3.21 to 3.16. Overall, the D_S profile performs slightly better than D_D in the 3D analyses, though the differences are small. It should also be noted that the 3D TTF amplitudes appear smoother and slightly reduced due to the application of Konno–Ohmachi smoothing (Konno and Ohmachi, 1998) to the FAS derived from the numerical simulations, whereas the 1D analytical TTFs are presented without smoothing, following the normal practice. While we have not yet implemented site-specific pseudo-3D D_S models in 3D GRAs at other downhole array sites, we plan to do so in the near future. In the present study, we used a full Rayleigh damping formulation in our 3D GRAs. However, recent 2D GRAs performed by our research group at other downhole array sites have shown strong dependency on the numerical damping formulation, with Rayleigh mass-only damping performing better than full Rayleigh or Maxwell damping formulations (Dawadi et al., 2025b). It will be interesting to combine site-specific D_S with Rayleigh mass-only damping in future 3D GRAs at downhole array sites in an attempt to better model ETFs.

6 CONCLUSIONS

This study presented preliminary results on the development of pseudo-3D models for both V_S and D_0 at the I-15 downhole array (I15DA) site in Salt Lake City, Utah, USA. The proposed models were based estimates of D_0 from laboratory-based empirical relationships and on in-situ estimates of D_0 obtained from surface wave testing, respectively. We validated both models by comparing the theoretical transfer functions under both 1D and 3D conditions with the observed amplification at the I15DA site. The validation demonstrated that 3D simulations significantly improve agreement with empirical data. This confirms the added value of H/V-based pseudo-3D models over conventional 1D assumptions. Indeed, including spatial variability and associated wave propagation phenomena, such as wave scattering, help to improve the reliability of the predicted site response. In addition, using in-situ estimates of the small-strain damping ratio further improved the match with the observed amplification, albeit with a more modest impact than observed for 1D simulations. This result shows the effectiveness of using in-situ estimates of the small-strain damping ratio from surface wave data for ground response analyses.

In-situ damping estimates are currently being refined, particularly to better fit high-frequency surface wave data. These improvements are expected to yield even more accurate damping ratio models, especially on the near-surface layers. These improvements will contribute to the development of more robust ground models for seismic site response assessments.

7 ACKNOWLEDGEMENTS

We would like to thank Jon Rusho from the University of Utah Seismograph Stations (UUSS) for providing the aftershock ground motions from the I15DA, which were used for computing ETFs to assess site response predictions. We would also like to thank David Stevens from the Utah Department of Transportation for helping to encourage care and maintenance of the I15DA.

8 REFERENCES

Abbas, A., Aimar, M., Cox, B.R., and Foti, S. 2025. A frequency-domain beamforming procedure for extracting Rayleigh wave attenuation coefficients and small-strain damping ratio from 2D

ambient noise array measurements. *Earthquake Spectra* 41(2), 1333-1363.

Aimar, M., Foti, S., and Cox, B.R. 2024a. Novel techniques for in situ estimation of shear-wave velocity and damping ratio through MASW testing – I: a beamforming procedure for extracting Rayleigh-wave phase velocity and phase attenuation. *Geophysical Journal International* 237(1), 506-524.

Aimar, M., Foti, S., and Cox, B.R. 2024b. Novel techniques for in situ estimation of shear-wave velocity and damping ratio through MASW testing part II: a Monte Carlo algorithm for the joint inversion of phase velocity and phase attenuation. *Geophysical Journal International* 237(1), 525-539.

Badsar, S.A. 2012. *In-Situ Determination of Material Damping in the Soil at Small Deformation Ratios (In situ bepaling van de materiaaldemping in de grond bij kleine vervormingen)*. PhD thesis, KU Leuven.

Darendeli, M.B. 2001. *Development of a new family of normalized modulus reduction and material damping curves*. PhD thesis, University of Texas at Austin.

Dawadi, N., Hallal, M.M., and Cox, B.R. 2024. Two-dimensional Ground Response Analyses at the Delaney Park Downhole Array Site. *Proc. 8th International Conference on Geotechnical Earthquake Engineering*,207-212.

Dawadi, N., Jackson, T.S., and Cox, B.R. 2025a. Three-Dimensional Ground Response Analyses at the I-15 Downhole Array Site near Salt Lake City. *Proc. Geo-Congress*.

Dawadi, N., Mohammadi, K., Hallal, M.M., and Cox, B.R. 2025b. Insights on Numerical Damping Formulations Gained from Calibrating Two-Dimensional Ground Response Analyses at Downhole Array Sites. *arXiv preprint* arXiv:2404.06650.

Falcone, G., Boldini, D., and Amorosi, A. 2018. Site response analysis of an urban area: A multi-dimensional and non-linear approach. *Soil Dynamics and Earthquake Engineering* 109, 33-45.

Foti, S., Hollender, F., Garofalo, F., Albarello, D., Asten, M., Bard, P.Y., Comina, C., Cornou, C., Cox, B.R., Di Giulio, G., Forbriger, T., Hayashi, K., Lunedei, E., Martin, A., Mercerat, D., Ohrnberger, M., Poggi, V., Renalier, F., Sicilia, D., and Socco, L.V. 2018. Guidelines for the good practice of surface wave analysis: a product of the InterPACIFIC project. *Bulletin of Earthquake Engineering* 16(6), 2367-2420.

Hallal, M.M., and Cox, B.R. 2021a. An H/V geostatistical approach for building pseudo-3D Vs models to account for spatial variability in ground response analyses Part I: Model development. *Earthquake Spectra*.

Hallal, M.M., and Cox, B.R. 2021b. An H/V geostatistical approach for building pseudo-3D Vs models to account for spatial variability in ground response analyses Part II: Application to 1D analyses at two downhole array sites. *Earthquake Spectra*.

Hallal, M.M., Cox, B.R., and Vantassel, J.P. 2022. Comparison of state-of-the-art approaches used to account for spatial variability in 1D ground response analyses. *Journal of Geotechnical and Geoenvironmental Engineering* 148(5).

Herrmann, R.B. 2013. Computer programs in seismology: An evolving tool for instruction and research. *Seismological Research Letters* 84, 1081-1088.

Jackson, T. 2024. *Evaluating 1D and 2D Small-Strain Ground Response Analyses at the I-15 Downhole Array Using Recorded Aftershocks from the M5.7 2020 Magna, Utah Earthquake*. Master's thesis, Utah State University.

Jackson, T.S., and Cox, B.R. 2025. A Database of Aftershock Ground Motions Recorded by the I-15 Downhole Array Following the 2020 M5.7 Magna, Utah Earthquake. *Proc. Geo Congress*.

Konno, K., and Ohmachi, T. 1998. Ground-motion characteristics estimated from spectral ratio between horizontal and vertical components of microtremor. *Bulletin of the Seismological Society of America* 88(1), 228-241.

Makra, K., and Chávez-García, F.J. 2016. Site effects in 3D basins using 1D and 2D models: an evaluation of the differences based on simulations of the seismic response of Euroseistest. *Bulletin of Earthquake Engineering* 14, 1177–1194.

Parolai, S., Lai, C.G., Dreossi, I., Ktenidou, O.J., and Yong, A. 2022. A review of near-surface QS estimation methods using active and passive sources. *Journal of Seismology* 26, 823-862.

Rathje, E.M., Kottke, A.R., and Trent, W.L. 2010. Influence of input motion and site property variabilities on seismic site response analysis. *Journal of Geotechnical and Geoenvironmental Engineering* 136(4), 607-619.

Teague, D.P., Cox, B.R., and Rathje, E.M. 2018. Measured vs. predicted site response at the garner valley downhole array considering shear wave velocity uncertainty from borehole and surface wave methods. *Soil Dynamics and Earthquake Engineering* 113, 339-355.

Wathelet, M., Jongmans, D., and Ohrnberger, M. 2004. Surface-wave inversion using a direct search algorithm and its application to ambient vibration measurements. *Near Surface Geophysics* 2(4), 211-221.

Wood, C.M., and Cox, B.R. 2012. A comparison of MASW dispersion uncertainty and bias for impact and harmonic sources. *Proc. GeoCongress 2012: State of the Art and Practice in Geotechnical Engineering*,2756-2765.

Youd, T.L., and Briggs, D.H. (2003) Downhole Seismic Array at The Intersection Of I-15, I-80 And SR-201, Salt Lake City, Utah. In.